Monsoon control on trace metal fluxes in the deep Arabian Sea

T M Balakrishnan Nair

Indian National Centre for Ocean Information Services (INCOIS), Ministry of Ocean Development, 'Ocean Valley', IDA–Jeedimetla (P.O), Hyderabad 500 055, India.
e-mail: bala@incois.gov.in

Particulate fluxes of aluminium, iron, magnesium and titanium were measured using six time-series sediment traps deployed in the eastern, central and western Arabian Sea. Annual Al fluxes at shallow and deep trap depths were 0.47 and 0.46 $g\,m^{-2}$ in the western Arabian Sea, and 0.33 and 0.47 $g\,m^{-2}$ in the eastern Arabian Sea. There is a difference of about 0.9–1.8 $g\,m^{-2}\,y^{-1}$ in the lithogenic fluxes determined analytically (residue remaining after leaching out all biogenic particles) and estimated from the Al fluxes in the western Arabian Sea. This arises due to higher fluxes of Mg (as dolomite) in the western Arabian Sea (6–11 times higher than the eastern Arabian Sea). The estimated dolomite fluxes at the western Arabian Sea site range from 0.9 to 1.35 $g\,m^{-2}\,y^{-1}$. Fe fluxes in the Arabian Sea were less than that of the reported atmospheric fluxes without any evidence for the presence of labile fraction/excess of Fe in the settling particles. More than 75% of Al, Fe, Ti and Mg fluxes occurred during the southwest (SW) monsoon in the western Arabian Sea. In the eastern Arabian Sea, peak Al, Fe, Mg and Ti fluxes were recorded during both the northeast (NE) and SW monsoons. During the SW monsoon, there exists a time lag of around one month between the increases in lithogenic and dolomite fluxes. Total lithogenic fluxes increase when the southern branch of dust bearing northwesterlies is dragged by the SW monsoon winds to the trap locations. However, the dolomite fluxes increase only when the northern branch of the northwesterlies (which carries a huge amount of dolomite accounting 60% of the total dust load) is dragged, from further north, by SW monsoon winds. The potential for the use of Mg/Fe ratio as a paleo-monsoonal proxy is examined.

1. Introduction

Atmospheric deposition of aerosols and mineral dust is a major pathway for the transport of trace elements and nutrients to the open ocean. The transport, quantity, chemistry and settling in the ocean surface are controlled by geological and atmospheric factors such as provenance of aerosols, wind velocity and direction, precipitation, etc. After deposition at the surface, the distribution and vertical flux of most of the trace elements are controlled by the production, sinking and deposition of the biogenic particles (Bruland *et al* 1994). Many studies on continental/lithogenic input of dust and trace elements to the marine environment revealed:

- that it can impact biogeochemical cycles and ocean productivity (Duce and Tindale 1991),
- the existence of a close correlation between the sedimentation of lithogenic and biogenic particles (Ittekkot *et al* 1991) and
- that it is essential to understand the connection between the present day deposition of elements and environmental factors before using the respective elements as potential proxies for paleo-oceanographic reconstructions (Shimmield and Mowbray 1991; Balakrishnan Nair *et al* 1999, 2005).

Keywords. Monsoon; fluxes; trace metal; Arabian Sea; aerosol; proxies.

J. Earth Syst. Sci. **115**, No. 4, August 2006, pp. 461–472

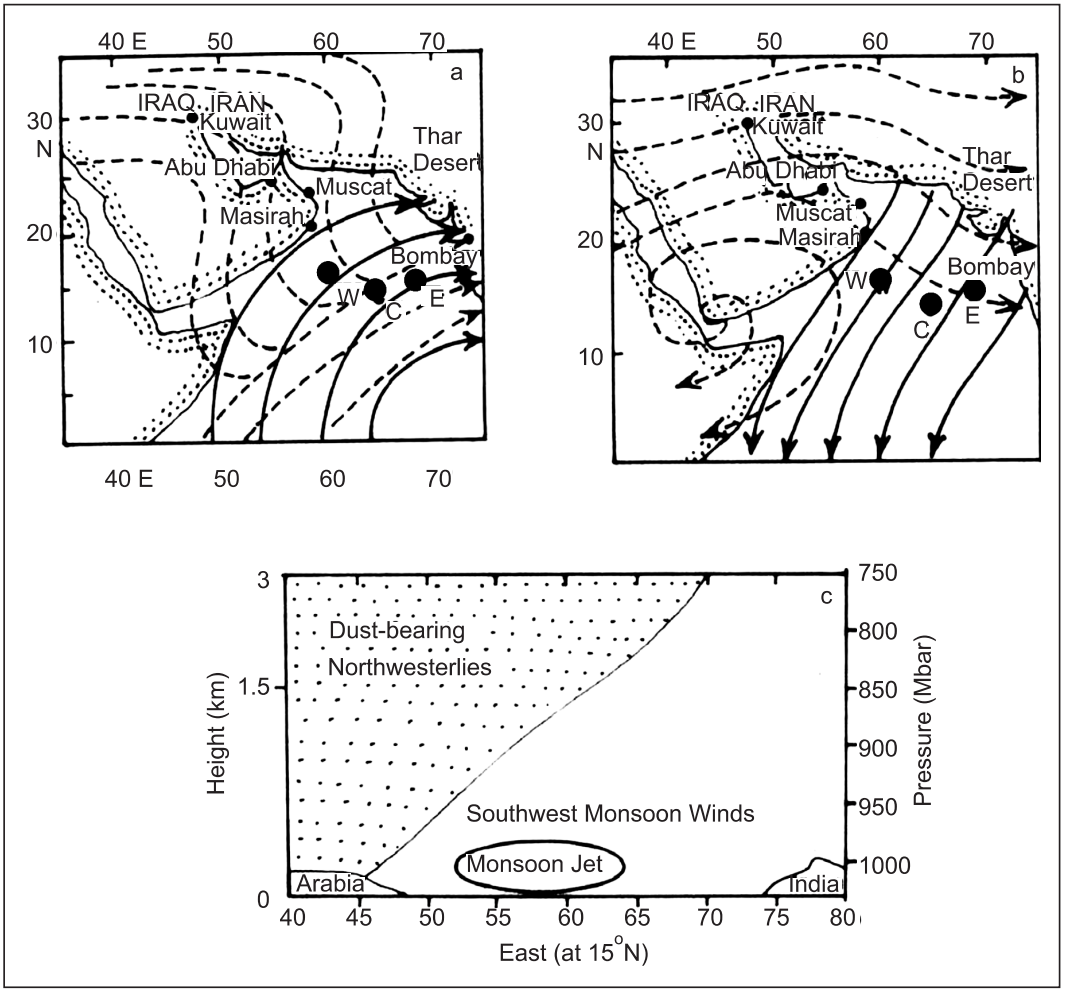

Figure 1. Locations of sediment traps in the Arabian Sea: W (WAST), C (CAST), E (EAST). Also shown is the wind pattern in the Arabian Sea. **(a)** Southwest monsoon winds (solid lines) over the Arabian Sea originating in the southern hemisphere and the dust-bearing northwesterly winds (dashed lines) which originate over the continents. Northwesterly winds meet and override the SW monsoon winds over the Arabian Sea. **(b)** NE monsoon winds (solid lines) and dust-bearing northwesterly winds (dashed lines). **(c)** Atmospheric profile (June, July, August) of the boundary between the dust bearing northwesterlies and the southwest monsoon winds along a transect at 15°N (after Clemens 1998).

Among the world oceans, the Arabian Sea is characterized by significantly high aeolian input (Duce *et al* 1991). The source areas of this dust are the northern tip of Persian Gulf near Iraq and Kuwait (Herman *et al* 1997), Thar desert (Ackerman and Cox 1989), inner desert and coastal regions of the Arabian peninsula (Herman *et al* 1997). This dust is transported by the northwesterlies over the Arabian peninsula. During summer monsoon, the northwesterlies override the moisture laden surface southwesterlies creating a sloping interference between two air masses, the monsoon inversion (figure 1). During winter or northeast (NE) monsoon winds carry dust to the Arabian Sea region. These monsoon winds transporting dust are found to be responsible for the spatial and seasonal variations in fluxes of particles in the Arabian Sea (Nair *et al* 1989; Rixen *et al* 1996). High aeolian input and seasonally varying particle flux patterns make the Arabian Sea an ideal site to study the trace metal fluxes and the mechanisms of transport. The main objective of the present paper is to study the spatial and seasonal variability of trace element fluxes in relation to monsoon winds.

2. Material and methods

PARFLUX Mark VI sediment traps have been deployed at three sites in the eastern (EAST; 15°58′N 69°36′E), central (CAST; 14°30′N 64°37′E) and western (WAST; 16°20′N 60°18′E) Arabian

Sea since May 1986. A total of 116 samples, collected between December 1992 and February 1994 from the above locations, have been analysed for the present study. Mooring locations are shown in figure 1. Prior to the deployment, the sampling cups were filled with filtered seawater from the mooring site and $HgCl_2(3.3\,g\,l^{-1})$ was added as a preservative to prevent bio-degradation of the trapped material.

Soon after recovery, the sediment trap samples were wet-sieved through a 1 mm mesh size nylon sieve, filtered onto pre-weighed 0.4 μm polycarbonate membrane filters, dried at 45°C and weighed to estimate total fluxes. Carbonate was determined with a Carmograph (Wustoff). Total carbon and nitrogen were analyzed using a Carlo-Erba 1500 Carbon-Nitrogen Analyzer. Organic carbon was determined as the difference between carbonate carbon and total carbon. Biogenic opal was determined spectrophotometrically based on a method modified from Mortlock and Froelich (1989).

For lithogenic and mineralogical analyses, 1/4 of the sample aliquot was treated with hydrogen peroxide and dilute acetic acid to remove organic matter and calcium carbonate, respectively. Biogenic silica was removed by heating the samples with 1 M solution of sodium carbonate at 90°C for two hours. Lithogenic fluxes were estimated by weighing the material remaining after the removal of biogenic carbonate, organic and opaline matter (for details, see Rixen *et al* 1996). Replicate analyses of all the samples showed that the variations were $< 1\%$ of the mean. The material remaining after the removal of these components was made into a thick slurry on a glass slide, dried and run on a Philips X-ray diffractometer from 3° to 35° 2θ at a scanning rate of 0.02° 2θ/sec using 40 kV and 20 mA settings and using a Ni-filtered Cu kα radiation. The peaks in the diffractogram at those given in brackets were used for mineral identification: Calcite (3.03Å), Feldspar (3.20Å), Quartz (4.26Å), Dolomite (2.89Å), Chlorite (4.53Å), Kaolinite + Chlorite (7.14Å), Palygorskite (10.16Å).

Sediment trap samples were digested with HNO_3, HF and $HClO_4$ mixture in a teflon beaker for geochemical analysis. Elemental determinations were carried out using a Perkin–Elmer Plasma-400 ICP-AES. Accuracies of the analyses were checked with a USGS standard (SGR-1) and found to be 2.7%, 5.9%, 3.6% and 2.6% for Fe, Al, Ti and Mg, respectively. Elemental fluxes were calculated by multiplying the elemental concentration with total flux. Mg_{excess} and Fe_{excess} (excess, with respect to crustal values) were calculated by the equation given by Murray and Leinen (1995)

$$\text{Element}_{\text{excess}} = \text{Element}_{\text{total}} - \left[\left(\frac{\text{Element}}{\text{Al}_{\text{crust}}}\right) \times \text{Al}_{\text{sample}}\right]$$

(crustal values were obtained from Taylor and McLennan 1985). Another way of estimating the excess over the crustal component is the Enrichment Factor (EF), which is given by

$$\text{EF} = \frac{(\text{Element/Al})_{\text{settling particles}}}{(\text{Element/Al})_{\text{crust}}}$$

(Zoller *et al* 1974; Jickells *et al* 1990).

3. Results and discussions

3.1 *Spatial variation of trace metal fluxes*

Aluminium is a major component of aluminosilicates (Taylor 1964). So, Al has been conventionally used to estimate the continental contribution to marine sediments (Shankar *et al* 1987; Saito *et al* 1992). Annual Al fluxes measured at shallow and deep trap depths were 0.47 and 0.46 $g\,m^{-2}$ in the western Arabian Sea and 0.33 and 0.47 $g\,m^{-2}$ in the eastern Arabian Sea (table 1). In the central Arabian Sea, fluxes were comparatively less ($0.26\,mg\,m^{-2}\,y^{-1}$) than at other stations because of the remoteness from the continents. The annual Al fluxes reported by Schussler *et al* (2005) in the central Arabian Sea during 1995 are higher ($0.38\,g\,m^{-2}\,y^{-1}$) than our values indicating an inter-annual variation in Al fluxes even in the central Arabian Sea. However, annual Al fluxes in the western Arabian Sea were less than the atmospheric Al flux reported for the Arabian Sea ($790\,mg\,m^{-2}\,y^{-1}$, Chester *et al* 1991). This discrepancy may be because of the spatial variation in sampling. In addition, annual atmospheric flux calculations were made from only two months of sampling by Chester *et al* (1991) in the Arabian Sea. In fact, sedimentation of aeolian particles is controlled by biogenic fluxes. Although the total annual fluxes were almost 3–4 times higher in the western Arabian Sea when compared to the eastern Arabian Sea, Al fluxes were almost comparable between the two regions. This implies that lithogenic content is more in particles settling in the eastern Arabian Sea. It is observed from the earlier studies that the percentage of lithogenic material (which is the source of detrital Al) is higher in the eastern Arabian Sea. Al fluxes reported are equivalent to $5.8\,g\,m^{-2}\,y^{-1}$ dust fluxes at the WAST and

Table 1. *Annual lithogenic and associated trace metal fluxes in the western (WAST), central (CAST) and eastern (EAST) parts of the Arabian Sea. Lithogenic and dolomite fluxes are in* $g\,m^{-2}\,y^{-1}$ *and trace metal fluxes are in mg* $m^{-2}\,y^{-1}$.

Station	Lith. flux		Al	Fe	Ti	Mg	$Mg_{exs.}$	$Mg_{exs.}$	Dolomite	
	Tot-bio	Al × 12.5	flux	flux	flux	flux	flux	%	Flux	%
WAST-919 m	6.68	5.79	463	310	27	353	176	50	1.35	20
WAST-2002 m	7.60	5.83	467	292	26	286	123	43	0.94	12
CAST-1042 m	3.47	3.24	259	187	14	154	56	37	0.43	12
CAST-2686 m	3.44	3.17	253	177	15	126	29	23	0.22	6
EAST-1632 m	4.15	4.09	327	237	20	153	29	19	0.22	5
EAST-2716 m	5.58	5.86	469	336	29	188	11	6	0.08	2
Atmospheric			790	560						

4–5.9 $g\,m^{-2}\,y^{-1}$ at the EAST site. There is a difference of about 0.9–1.7 $g\,m^{-2}\,y^{-1}$ between the lithogenic fluxes obtained with the analytical method (total flux – biogenic flux) and that estimated from the Al fluxes (assuming that Al content in the lithogenic matter is 8.04% as in the upper continental crust). This difference is significant in the western Arabian Sea compared to the central and eastern regions. This suggests a mineralogical differentiation in the lithogenic component in the western Arabian Sea. This is because of the higher flux of Mg_{excess} to the western Arabian Sea than to the eastern part.

Magnesium in the marine environment is obtained from biogenic or aeolian sources. Calcite materials contain variable Mg content. Calcites are classified, based on their degree of Mg content, as low-Mg calcite (3–4% $MgCO_3$), high-Mg calcite (5–16% $MgCO_3$) and dolomite (>16% $MgCO_3$). Generally, high-Mg calcite is secreted by calcareous algae, which are restricted to the near-shore environment. Since the biogenic component of Mg is removed through acid leaching, the Mg_{excess} observed in our samples is presumed to be from non-biogenic sources. Mg fluxes show that 50% Mg are in excess in the western Arabian Sea as compared to less than 20% in the eastern part (table 1). The Mg_{excess} fluxes in the western Arabian Sea are 6–11 times higher than the eastern Arabian Sea though the lithogenic fluxes are comparable. Mg_{excess} can be contributed by Mg-rich montmorillonite. However, the flux of montmorillonite is very less in the western Arabian Sea (Ramaswamy *et al* 1991). The present study also does not indicate the presence of montmorillonite. Further, mineralogical studies confirm the presence of dolomite (figure 2) in the western Arabian Sea trap samples. Estimated dolomite fluxes (assuming that the entire Mg_{excess} fluxes are in the mineral form of dolomite) at the western Arabian Sea site range from 0.94 to 1.35 $g\,m^{-2}\,y^{-1}$. Dolomite flux more or less compensates for the discrepancy observed between the estimation of lithogenic fluxes from Al fluxes and weight loss methods. The dolomite fluxes comprise ∼ 20% of lithogenic fluxes in the western Arabian Sea. Dolomite may be preferentially transported by the westerlies since the dolomite-containing Mesozoic strata are exposed only in northern Arabia. Some dolomite may also have come from the *Subka* sediments around the Persian Gulf. The aeolian material from these source areas can be enriched with dolomite. Tindale and Pease (1999), revealed that aerosols over the western Arabian Sea and silt/clay samples (collected from deserts and *Wadis* in coastal Oman) have as much as 30% of carbonate material.

Iron fluxes are important in the marine environment as it is a critical element for the growth of phytoplankton (Martin and Fitzwater 1988). Productivity in high nutrient and low chlorophyll regions, such as the Southern Ocean or the equatorial Pacific Ocean, is controlled by Fe input from aerosols. Iron also enhances export production and reduces the atmospheric carbon dioxide (Kumar *et al* 1995). The flux of Fe is comparable between the eastern and western Arabian Sea regions. The flux was ∼ 0.3 $g\,m^{-2}\,y^{-1}$ at the western Arabian Sea and had a range of 0.24–0.34 $g\,m^{-2}\,y^{-1}$ in the eastern Arabian Sea (table 1). Fluxes were comparatively less in the central Arabian Sea mainly because the site is at a distance from the landmasses. The atmospheric Fe flux is ∼ 560 $mg\,m^{-2}\,y^{-1}$ over the Arabian Sea (Chester *et al* 1991) which is higher than the Fe flux (310 $mg\,m^{-2}\,y^{-1}$) in the traps at 900 m in the western Arabian Sea. This discrepancy may be attributed to spatial and seasonal variability in sampling (Chester *et al* (1991) sampled aerosols during the NE monsoon from both coastal and open ocean regions). As the solubility of Fe (from aerosols) in the Arabian Sea water

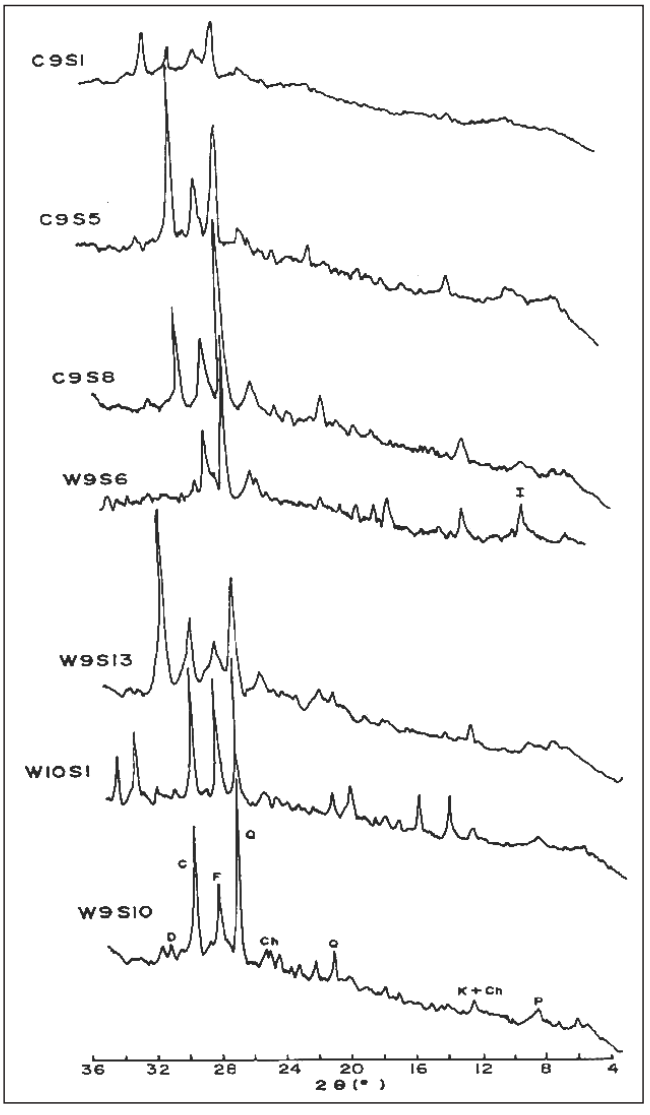

Figure 2. X-ray diffractograms of the lithogenic fraction of sediment trap samples from the central (C9S1, C9S5 & C9S8) and western (W9S6, W9S13, W10S1 & W9S10) Arabian Sea. Prominent peaks identified are: D – Dolomite; C – Calcite; F – Feldspar; Q – Quartz; Ch – Chlorite; K – Kaolinite; P – Palygorskite; I – Illite.

is negligible (<1% of total deposition, Chester *et al* 1991), one may consider that the settling Fe flux should be nearly equal to the atmospheric Fe flux. The aerosol studies further indicate that the atmospheric aqueous labile (water soluble) Fe concentration during the inter monsoon range between 0.4 and 4.75 ng m^{-3} but is below detection level during the SW monsoon period (Siefert *et al* 1999). However, our results do not show any evidence of Fe_{excess} fluxes indicating that the labile fraction gets utilised by organisms or get dissolved in Oxygen Minimum Zone, and that the Fe associated with the mineral phase is only settling below. The fluxes of Ti also show the same spatial variation as Fe. It varies from 26 to 27 mg m^{-2} y^{-1} in WAST and 20 to 28 mg m^{-2} y^{-1} in the EAST traps. Annual flux of Al, Fe and Ti shows an increase with depth in the eastern Arabian Sea. It may be because of the resuspension and lateral transport from the eastern continental slope of the Arabian Sea (Ramaswamy *et al* 1991).

3.2 *Seasonal variation in trace metal fluxes*

Seasonal variations in elemental fluxes are shown in table 2A–C. More than 75% of the Al, Fe, Ti and Mg fluxes were registered during the SW monsoon in the western Arabian Sea. In the eastern Arabian Sea, peak Al, Fe, Mg and Ti fluxes were recorded during both NE and SW monsoons.

Concentrations of Al and Fe show an excellent correlation indicating the absence of mineralogical differentiation or biological addition for these elements. This is also seen in seasonal patterns in Enrichment Factors (EF), which is near to 1 during all the seasons indicating the crustal contribution without much mineralogical differentiation (figure 3). However, the EF of Mg shows seasonally varying pattern with higher values during the NE and SW monsoon seasons. This indicates the deposition of Mg bearing carbonates such as dolomite during the SW monsoon season. The mineralogical analysis indicates that the dolomite peaks are the most prominent in samples (W9S13) of the SW monsoon period (figure 2). Moreover, distinct peaks of coarse grains, such as quartz and calcite, are also observed during the SW monsoon period. Obviously, increased atmospheric deposition and biological scavenging account for increased fluxes in the SW monsoon period. According to Sirocko (1993), 91% of the annual dust transport to the western Arabian Sea occurs during June–August and is controlled by monsoon winds. These observations are supported by the recent remote sensing data, which indicate the highest annual mean of Estimated Aerosol Optical Thickness (EAOT = 0.32) over the Arabian Sea (Husar *et al* 1997). The EAOT peaks sharply during June, July and August (EAOT = 0.61–0.65). Li and Ramanathan (2002) also reported that maximum monthly mean value of Aerosol Optical Depth during SW monsoon (~ 0.6) is three times higher than in the NE monsoon (~ 0.2). However, other studies indicate that the dust levels are generally lower over the Arabian Sea during summer than in other seasons (Tindale and Pease 1999). According to them, the Findlater jet (a strong, low level, atmospheric jet associated with the SW monsoon), rather than acting as a source of dust from Africa (see figure 1), appears to block the direct transport of dust to the open Arabian Sea from desert dust source regions in the Middle East

Table 2(A). *Lithogenic and associated elemental fluxes in the western Arabian Sea. Lithogenic, Al, Fe and Mg fluxes are in mg m^{-2} d^{-1} and Ti flux is in μg m^{-2} d^{-1}.*

Sampling duration	Sample ID	Lithog. flux (Total bio.flux)	Lithog. flux (Al flux ×12.5)	Al flux	Ti flux	Fe flux	Mg flux	$Mg_{exs.}$ flux	Dolomite Flux	Dolomite %
WAST-919 m										
20-01-93 to 15-02-93	W9S2	2.62	1.15	0.09	6.42	0.05	0.07	0.03	0.23	8.8
15-02-93 to 13-03-93	W9S3	4.03	5.55	0.44	24.25	0.38	0.28	0.11	0.85	21.0
13-03-93 to 08-04-93	W9S5	11.37	9.17	0.73	36.59	0.62	0.47	0.19	1.42	12.5
08-04-93 to 04-05-93	W9S6	11.69	15.41	1.23	68.15	0.82	0.69	0.22	1.71	14.6
04-05-93 to 30-05-93	W9S7	13.09	12.37	0.99	39.93	0.67	0.78	0.41	3.12	23.8
30-05-93 to 25-06-93	W9S8	14.80	14.59	1.17	60.55	0.83	1.03	0.59	4.49	30.3
25-06-93 to 21-07-93	W9S9	36.66	29.47	2.36	135.38	1.56	1.43	0.53	4.05	11.1
21-07-93 to 04-08-93	W9S10	84.67	93.38	7.47	455.08	5.37	6.56	3.71	28.42	33.6
04-08-93 to 17-08-93	W9S11	36.24	35.20	2.82	186.17	1.85	1.91	0.84	6.43	17.7
17-08-93 to 30-08-93	W9S12	27.89	30.01	2.40	154.31	1.14	2.17	1.26	9.64	34.6
30-08-93 to 12-09-93	W9S13	10.05	22.58	1.81	102.26	0.93	1.47	0.78	5.97	59.5
18-10-93 to 14-11-93	W10S1	17.03	11.82	0.95	57.84	0.68	0.59	0.23	1.78	10.5
14-11-93 to 11-12-93	W10S2	24.05	11.34	0.91	49.46	0.63	0.64	0.30	2.27	9.4
11-12-93 to 07-01-94	W10S3	18.65	11.24	0.90	51.58	0.60	0.57	0.22	1.71	9.2
07-01-94 to 03-02-94	W10S4	16.22	5.84	0.47	27.00	0.30	0.34	0.16	1.21	7.5
03-02-94 to 02-03-94	W10S5	12.53	5.65	0.45	23.50	0.28	0.50	0.32	2.48	19.8
Average		**21.35**	**19.67**	**1.57**	**92.40**	**1.04**	**1.22**	**0.62**	**4.74**	**20.2**
WAST-2002 m										
25-12-92 to 20-01-93	W9M13	10.58	11.73	0.94	56.30	0.55	0.64	0.29	2.20	20.8
20-01-93 to 15-02-93	W9M12	22.41	10.53	0.84	50.79	0.45	0.92	0.60	4.57	20.4
15-02-93 to 13-03-93	W9M11	24.22	13.40	1.07	58.14	0.92	0.78	0.37	2.83	11.7
13-03-93 to 08-04-93	W9M10	19.21	10.95	0.88	51.55	0.50	0.60	0.26	2.02	10.5
08-04-93 to 04-05-93	W9M9	17.02	–	–	–	–	–	–	–	–
04-05-93 to 30-05-93	W9M8	13.08	8.83	0.71	44.86	0.44	0.51	0.24	1.86	14.2
30-05-93 to 25-06-93	W9M7	14.87	18.36	1.47	84.61	0.99	1.03	0.47	3.57	24.0
25-06-93 to 21-07-93	W9M6	35.67	38.56	3.09	152.47	2.15	1.99	0.82	6.25	17.5
21-07-93 to 16-08-93	W9M5	6.12	14.24	1.14	62.31	0.82	0.64	0.21	1.61	26.3
16-08-93 to 29-08-93	W9M4	36.42	52.00	4.16	329.27	2.97	2.41	0.82	6.29	17.3
29-08-93 to 24-09-93	W9M3	11.49	26.14	2.09	119.89	1.43	1.47	0.67	5.16	44.9
24-09-93 to 11-10-93	W9M2	–	0.27	0.02	1.18	0.01	0.01	0.00	0.03	–
18-10-93 to 14-11-93	W10M1	24.61	13.15	1.05	68.77	0.80	0.71	0.31	2.37	9.6
14-11-93 to 11-12-93	W10M2	16.66	13.00	1.04	62.04	0.76	0.67	0.27	2.09	12.6
11-12-93 to 07-01-94	W10M3	20.36	9.81	0.78	39.98	0.51	0.46	0.16	1.25	6.1
07-01-94 to 03-02-94	W10M4	23.57	12.77	1.02	59.42	0.69	0.59	0.20	1.51	6.4
03-02-94 to 02-03-94	W10M5	22.41	11.84	0.95	9.96	0.64	0.56	0.20	1.55	6.9
Average		**19.75**	**16.92**	**1.35**	**82.77**	**0.93**	**0.90**	**0.38**	**2.91**	**17.3**

and Iran/Pakistan. The present study, nevertheless, reveals increased dolomite fluxes associated with the coarse fraction of the aerosols during the SW monsoon. The CAST is located almost at the centre whereas EAST is still to the east of the axis of the Findlater jet. However, EF during the beginning of the SW monsoon is equal (EF = 1.8) to that in aerosols originated over the Arabian continent (figure 3). Moreover, the prominent crystalline materials such as quartz, calcite and feldspar, etc. were also observed in the CAST samples during the SW monsoon (figure 2). This reveals that the coarse grained material actually deposited up to the eastern region of the Arabian Sea during SW monsoon. During summer monsoon, surface winds over the Arabian Sea originate in the southern hemisphere whereas winds aloft (northwesterlies) are from the dust source area in the north (figure 1). Thus the presence of coarse-grained dolomite in all the trap samples during the SW monsoon indicates the deposition from the air mass aloft the Findlater jet.

Though there is a sharp (~ 2 fold) increase in the lithogenic flux from early June to mid-July, dolomite fluxes increase (7 fold) only between late July and early August (table 2A, samples

Table 2(B). *Lithogenic and associated elemental fluxes in the central Arabian Sea. Lithogenic, Al, Fe and Mg fluxes are in mg m^{-2} d^{-1} and Ti flux is in μg m^{-2} d^{-1}.*

Sampling duration	Sample ID	Lithog. flux (Total bio.flux)	Lithog. flux (Al flux ×12.5)	Al flux	Ti flux	Fe flux	Mg flux	$Mg_{exs.}$ flux	Dolomite Flux	Dolomite %
CAST-1042 m										
25-12-92 to 20-01-93	C9S1	5.72	7.97	0.64	35.19	–	–	0.18	1.40	24.5
20-01-93 to 15-02-93	C9S2	8.35	7.50	0.60	33.62	0.42	0.35	0.12	0.92	11.0
15-02-93 to 13-03-93	C9S3	7.91	8.41	0.67	37.03	0.49	0.43	0.16	1.22	15.4
13-03-93 to 08-04-93	C9S4	7.37	5.88	0.47	26.02	0.38	0.28	0.07	0.54	7.3
08-04-93 to 04-05-93	C9S5	6.44	6.81	0.54	29.04	0.48	0.32	0.08	0.62	9.6
04-05-93 to 30-05-93	C9S6	5.87	5.24	0.42	24.66	0.39	0.26	0.07	0.54	9.2
30-05-93 to 25-06-93	C9S7	7.38	8.70	0.70	42.70	0.61	0.44	0.12	0.96	12.9
25-06-93 to 21-07-93	C9S8	20.55	15.44	1.23	60.51	0.87	0.94	0.47	3.63	17.7
21-07-93 to 03-08-93	C9S9	8.81	8.06	0.65	38.43	0.51	0.42	0.14	1.06	12.1
03-08-93 to 16-08-93	C9S10	–	–	–	–	–	–	–	–	–
16-08-93 to 29-08-93	C9S11	–	–	–	–	–	–	–	–	–
29-08-93 to 11-09-93	C9S12	–	–	–	–	–	–	–	–	–
11-09-93 to 24-09-93	C9S13	–	–	–	–	–	–	–	–	–
18-10-93 to 14-11-93	C10S1	11.18	10.05	0.80	46.97	0.67	0.64	0.33	2.52	22.5
14-11-93 to 11-12-93	C10S2	7.80	8.11	0.65	37.98	0.46	0.28	0.04	0.28	3.6
11-12-93 to 07-01-94	C10S3	11.71	9.53	0.76	42.74	0.54	0.44	0.15	1.15	9.8
07-01-94 to 03-02-94	C10S4	9.38	7.89	0.63	35.02	0.43	0.35	0.11	0.87	9.3
03-04-94 to 02-03-94	C10S5	9.74	8.70	0.70	37.96	0.50	0.34	0.08	0.60	6.1
Average	–	**9.16**	**8.45**	**0.68**	**37.70**	**0.52**	**0.43**	**0.16**	**1.19**	**11.7**
CAST-2878 m										
25-12-92 to 07-01-93	C9D1	4.59	4.90	0.39	26.98	–	–	0.05	0.35	7.6
07-01-93 to 20-01-93	C9D2	3.02	6.62	0.53	32.09	0.41	0.27	0.06	0.49	16.1
20-01-93 to 02-02-93	C9D3	4.88	5.96	0.48	33.83	0.36	0.23	0.05	0.40	8.3
02-02-93 to 15-02-93	C9D4	6.43	7.17	0.57	31.70	0.40	0.29	0.07	0.52	8.1
15-02-93 to 28-02-93	C9D5	7.26	6.50	0.52	33.35	0.39	0.27	0.07	0.55	7.6
28-02-93 to 13-03-93	C9D6	7.79	6.99	0.56	33.67	0.39	0.26	0.05	0.37	4.8
13-03-93 to 26-03-93	C9D7	9.68	9.54	0.76	45.33	0.55	0.44	0.15	1.14	11.8
26-03-93 to 08-04-93	C9D8	6.78	6.52	0.52	34.65	0.39	0.25	0.05	0.39	5.8
08-04-93 to 21-04-93	C9D9	6.53	7.55	0.60	33.93	0.42	0.27	0.04	0.30	4.7
21-04-93 to 03-05-93	C9D10	7.08	6.44	0.52	30.50	0.37	0.23	0.03	0.24	3.4
04-05-93 to 17-05-93	C9D11	8.12	7.45	0.60	38.85	–	–	0.04	0.32	3.9
17-05-93 to 30-05-93	C9D12	8.54	8.42	0.67	43.11	0.50	0.28	0.03	0.21	2.4
30-05-93 to 12-06-93	C9D13	5.68	5.17	0.41	26.72	0.30	0.19	0.03	0.22	3.9
12-06-93 to 25-06-93	C9D14	5.87	7.36	0.59	36.87	0.44	0.26	0.03	0.24	4.1
25-06-93 to 08-07-93	C9D15	2.38	4.49	0.36	23.45	0.26	0.17	0.03	0.25	10.7
08-07-93 to 21-07-93	C9D16	8.77	8.03	0.64	40.20	0.51	0.32	0.08	0.58	6.7
21-07-93 to 03-08-93	C9D17	9.72	8.19	0.66	40.66	0.47	0.31	0.06	0.43	4.4
03-08-93 to 16-08-93	C9D18	15.63	11.08	0.89	57.00	0.59	0.48	0.15	1.12	7.2
16-08-93 to 29-08-93	C9D19	–	–	–	–	–	–	–	–	–
29-08-93 to 11-09-93	C9D20	–	–	–	–	–	–	–	–	–
11-09-93 to 24-09-93	C9D21	–	–	–	–	–	–	–	–	–
18-10-93 to 14-11-93	C10D1	12.07	8.81	0.70	39.92	0.47	0.59	0.32	2.46	20.4
14-11-93 to 11-12-93	C10D2	12.96	10.26	0.82	49.51	0.55	0.36	0.04	0.33	2.6
11-12-93 to 24-12-94	C10D3	12.35	8.60	0.69	40.54	0.44	0.30	0.03	0.26	2.1
24-12-93 to 07-01-94	C10D4	25.61	17.65	1.41	83.63	0.91	0.65	0.11	0.86	3.4
07-01-94 to 20-01-94	C10D5	14.11	11.89	0.95	55.42	0.64	0.44	0.08	0.58	4.1
Average		**8.95**	**8.07**	**0.65**	**39.65**	**0.53**	**0.40**	**0.10**	**0.79**	**7.2**

Table 2(C). *Lithogenic and associated elemental fluxes in the eastern Arabian Sea. Lithogenic, Al, Fe and Mg fluxes are in mg m^{-2} d^{-1} and Ti flux is in μg m^{-2} d^{-1}.*

Sampling duration	Sample ID	Lithog. flux (Total bio.flux)	Lithog. flux (Al flux ×12.5)	Al flux	Ti flux	Fe flux	Mg flux	$Mg_{exs.}$ flux	Dolomite Flux	Dolomite %
EAST-1632 m										
10-12-92 to 24-12-92	E9S1	23.59	33.47	2.68	184.73	1.94	1.18	0.16	1.20	5.1
24-12-92 to 07-01-93	E9S2	25.96	21.10	1.69	108.78	1.21	1.13	0.48	3.69	14.2
07-01-93 to 21-01-93	E9S3	27.47	22.17	1.77	114.70	1.37	0.86	0.19	1.43	5.2
21-01-93 to 04-02-93	E9S4	21.82	18.83	1.51	91.36	1.07	0.93	0.35	2.70	12.4
04-02-93 to 18-02-93	E9S5	26.08	17.70	1.42	104.11	1.09	0.68	0.14	1.10	4.2
18-02-93 to 04-03-93	E9S6	11.33	7.24	0.58	37.79	0.43	0.25	0.03	0.23	2.0
04-03-93 to 18-03-93	E9S7	5.99	13.86	1.11	76.10	0.87	0.57	0.15	1.16	19.4
18-03-93 to 01-04-93	E9S8	–	–	–	–	–	–	–	–	–
01-04-93 to 15-04-93	E9S9	5.91	8.55	0.68	44.17	0.51	0.38	0.12	0.94	15.9
15-04-93 to 29-04-93	E9S10	4.52	3.57	0.29	18.57	0.21	0.12	0.01	0.06	1.4
29-04-93 to 13-05-93	E9S11	6.21	5.02	0.40	25.41	0.30	0.18	0.03	0.21	3.4
13-05-93 to 27-05-93	E9S12	3.85	3.73	0.30	19.27	0.23	0.12	0.01	0.08	2.1
27-05-93 to 10-06-93	E9S13	10.60	9.29	0.74	48.77	0.55	0.32	0.04	0.30	2.8
10-06-93 to 24-06-93	E9S14	5.88	4.28	0.34	19.85	0.24	0.22	0.09	0.69	11.7
24-06-93 to 08-07-93	E9S15	4.18	6.64	0.53	31.60	0.39	0.21	0.00	0.03	0.6
08-07-93 to 22-07-93	E9S16	–	–	–	–	–	–	–	–	–
22-07-93 to 05-08-93	E9S17	–	–	–	–	–	–	–	–	–
05-08-93 to 19-08-93	E9S18	–	–	–	–	–	–	–	–	–
19-08-93 to 02-09-93	E9S19	5.13	5.14	0.41	25.51	0.29	0.17	0.01	0.07	1.3
02-09-93 to 16-09-93	E9S20	26.67	24.52	1.96	120.99	1.41	0.80	0.06	0.43	1.6
18-10-93 to 14-11-93	E10S1	9.65	17.10	1.37	84.88	0.97	0.63	0.10	0.80	8.3
14-11-93 to 11-12-93	E10S2	17.81	10.66	0.85	51.09	0.59	0.37	0.04	0.34	1.9
11-12-93 to 07-01-94	E10S3	3.66	6.70	0.54	31.16	0.36	0.21	0.00	0.02	0.6
07-01-94 to 03-02-94	E10S4	23.45	10.02	0.80	43.94	0.56	0.34	0.04	0.28	1.2
03-02-94 to 02-03-94	E10S5	25.31	5.11	0.41	23.02	0.28	0.17	0.01	0.11	0.4
Average		**14.05**	**12.13**	**0.97**	**62.18**	**0.56**	**0.34**	**0.04**	**0.30**	**3.2**
EAST-2716 m										
10-12-92 to 24-12-92	E9D1	20.53	30.72	2.46	151.39	1.70	0.97	0.04	0.27	1.3
24-12-92 to 07-01-93	E9D2	13.11	19.34	1.55	92.60	1.06	0.60	0.01	0.07	0.6
07-01-93 to 21-01-93	E9D3	14.66	18.22	1.46	93.42	1.07	0.59	0.04	0.28	1.9
21-01-93 to 04-02-93	E9D4	13.68	11.71	0.94	68.70	0.66	0.37	0.02	0.13	1.0
04-02-93 to 18-02-93	E9D5	16.43	18.75	1.50	96.54	1.06	0.60	0.03	0.22	1.4
18-02-93 to 04-03-93	E9D6	6.65	9.10	0.73	48.12	0.60	0.31	0.03	0.26	3.9
04-03-93 to 18-03-93	E9D7	9.62	6.83	0.55	34.08	0.39	0.37	0.16	1.25	13.0
18-03-93 to 01-04-93	E9D8	11.91	13.47	1.08	66.67	0.77	0.40	–	–	–
01-04-93 to 15-04-93	E9D9	7.54	6.44	0.52	32.20	0.40	0.21	0.01	0.09	1.1
15-04-93 to 29-04-93	E9D10	6.30	4.28	0.34	22.54	0.28	0.18	0.05	0.41	6.5
29-04-93 to 13-05-93	E9D11	9.35	7.61	0.61	38.72	0.46	0.25	0.01	0.11	1.2
13-05-93 to 27-05-93	E9D12	5.57	9.89	0.79	50.84	0.60	0.30	–	–	–
27-05-93 to 10-06-93	E9D13	5.75	7.53	0.60	33.80	0.44	0.24	0.01	0.10	1.7
10-06-93 to 24-06-93	E9D14	10.43	9.87	0.79	49.40	0.60	0.35	0.05	0.35	3.4
24-06-93 to 08-07-93	E9D15	7.82	19.26	1.54	90.64	1.19	0.62	0.03	0.26	3.4
08-07-93 to 22-07-93	E9D16	7.31	4.21	0.34	20.87	0.25	0.15	0.02	0.19	2.6
22-07-93 to 05-08-93	E9D17	11.71	11.64	0.93	59.47	0.72	0.50	0.15	1.14	9.8
05-08-93 to 19-08-93	E9D18	8.45	12.59	1.01	59.27	0.73	0.39	0.01	0.05	0.6
19-08-93 to 02-09-93	E9D19	12.91	14.46	1.16	72.13	0.84	0.47	0.03	0.22	1.7
03-09-93 to 16-09-93	E9D20	24.68	24.61	1.97	112.38	1.45	0.77	0.02	0.12	0.5
18-10-93 to 14-11-93	E10D1	31.94	33.12	2.65	150.63	1.81	1.01	–	–	–
14-11-93 to 11-12-93	E10D2	19.95	19.81	1.58	97.37	1.08	0.61	0.00	0.01	0.1
11-12-93 to 24-12-93	E10D3	20.24	20.89	1.67	102.34	1.12	0.67	0.03	0.22	1.1
24-12-93 to 07-01-94	E10D4	23.45	15.42	1.23	77.25	0.89	0.48	0.02	0.12	0.5
07-01-94 to 20-01-94	E10D5	25.31	25.00	2.00	120.81	1.47	0.77	0.00	0.04	0.1
Average	–	**13.81**	**14.99**	**1.20**	**73.69**	**0.80**	**0.45**	**0.03**	**0.24**	**2.4**

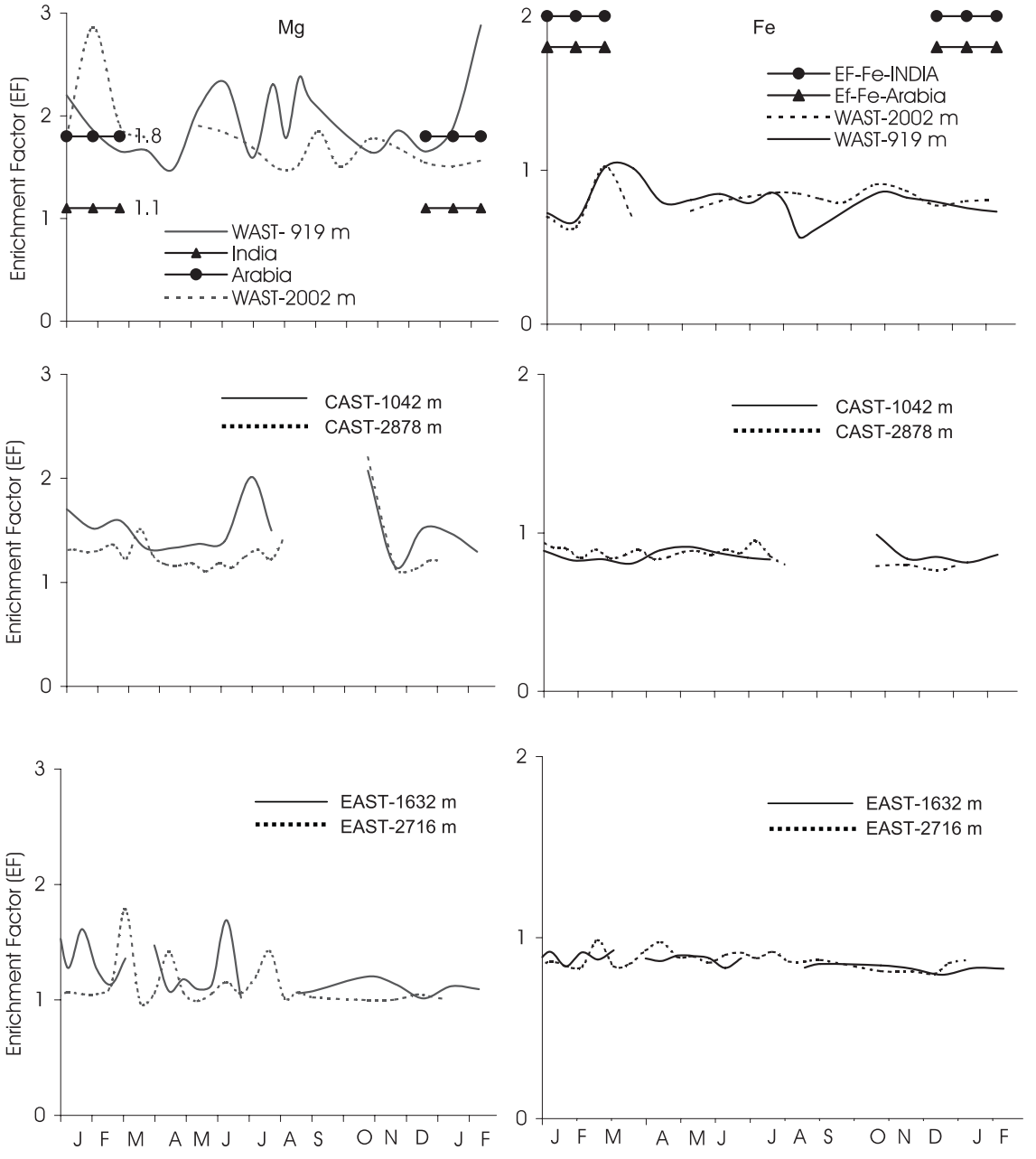

Figure 3. Monthly variation of Enrichment Factor (EF) of Mg, Ti and Fe in the settling particles from the western (WAST), central (CAST) and eastern (EAST) Arabian Sea. EF of these elements in the aerosols are identified with the aerosol trajectories originating from India and the Arabian peninsula. EF data for aerosols are from Johansen and Hoffmann (2003).

W9S8-W9S10). Thus, there is a time lag of around one month between the increases in lithogenic and dolomite fluxes. The dolomite contributed up to 60% of lithogenic fluxes at the end of the SW monsoon period. In agreement with this, 2-fold differences between the lithogenic fluxes calculated by the weight loss method and estimated from the Al fluxes (table 2A; samples W9S13 and W9M3) was observed. Thus it can be inferred that there is a distinct change in the provenance of lithogenic material deposited in the Arabian Sea between the early and late SW monsoon. The cause for this variation is the shift of Inter-Tropical Convergence Zone (ITCZ). As the SW monsoon progresses, the boundary between the dust-bearing northwesterlies and the SW monsoon winds, the ITCZ, shifts towards north (figure 1). Finer particles like clay may be more abundant at the southern end of the westerlies which may be diverted to the trap locations during June, which causes a general increase in lithogenic fluxes. The northern branch of the northwesterlies carries a huge amount of dolomite which accounts for 60% of the total dust load (sampled in Kuwait;

Khalaf 1989). These dust loads may be diverted to the western trap location only when the SW monsoon winds drag the westerlies from further north.

3.3 *Mineralogy of sediment trap samples*

X-ray diffractograms of the sediment trap samples indicate the presence of prominent clay minerals like chlorite, illite and palygorskite (figure 2). Palygorskite is present mainly in the western Arabian Sea trap samples (W9S6, W10S1 and W9S10). It forms in semi-arid, hot environments with changing ground water levels that occur in the *Subka* and *Wadi* deposits (Al Saayari and Zotl 1978). The presence of palygorskite in the western Arabian Sea has been reported by Ramaswamy *et al* (1991) and the present results confirm this report. In addition to the above-mentioned sources, the Mesozoic rocks of the Arabian peninsula may also supply large amounts of detrital palygorskite (Muller 1961). Illite is the major clay mineral in all the trap samples (Ramaswamy *et al* 1991). Illite may have been derived from the Indus River (Konta 1985) and/or aeolian dust (Chester *et al* 1985). Prominent crystalline minerals present are quartz, feldspars, calcite, and dolomite. Fine-grained detrital quartz may form by the chemical and physical weathering of non-alkaline rocks, especially of granite and clastic sediments. Calcite peaks are prominent in the western and central Arabian Sea trap samples. As biogenic calcite has already been removed, the peaks may represent lithogenic calcite which is not easily removed by acetic acid treatment.

3.4 *Paleo-monsoon implications*

The aerosols collected over Kuwait show that Fe oxide comprises a major portion of the fine particles (Khalaf 1989). As Fe oxides may be transported as far as 3300 km from the African coast (Balsam *et al* 1995), they necessarily have to be fine sized. The association of dolomite with the coarse fraction and of Fe oxide with the fine fraction makes Mg/Fe ratio a potential proxy for wind intensity and direction in the western Arabian Sea. Mg/Fe ratios are high during both the NE and late SW monsoons (figure 4). Although wind velocity during the NE monsoon is very low when compared to that of SW monsoon, Mg/Fe ratios are still comparable or slightly higher during the NE monsoon indicating that wind direction is indeed responsible for the high Mg/Fe ratios.

Conservative element such as Ti is considered to be contributed by heavy minerals, such as rutile, and anatase (both TiO_2; e.g., Delany *et al* 1967; Schutz and Rahn 1982). The ratios of Ti/Al should mainly reflect grain size and would therefore be

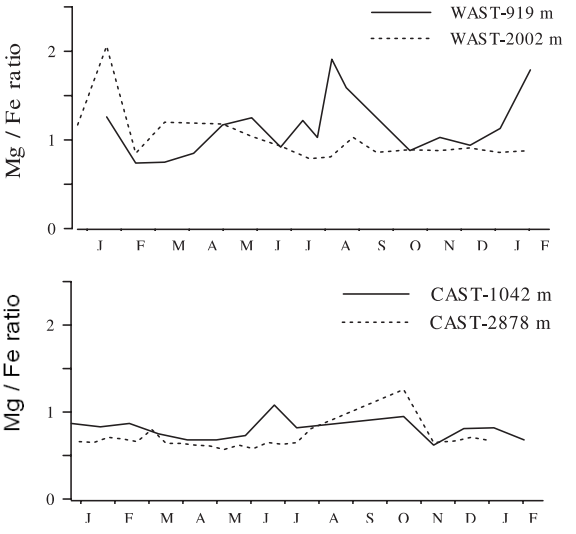

Figure 4. Seasonal variation of Mg/Fe in the sediment traps samples in the western (WAST) and central (CAST) Arabian Sea. Note high ratios during the NE and late southwest monsoons.

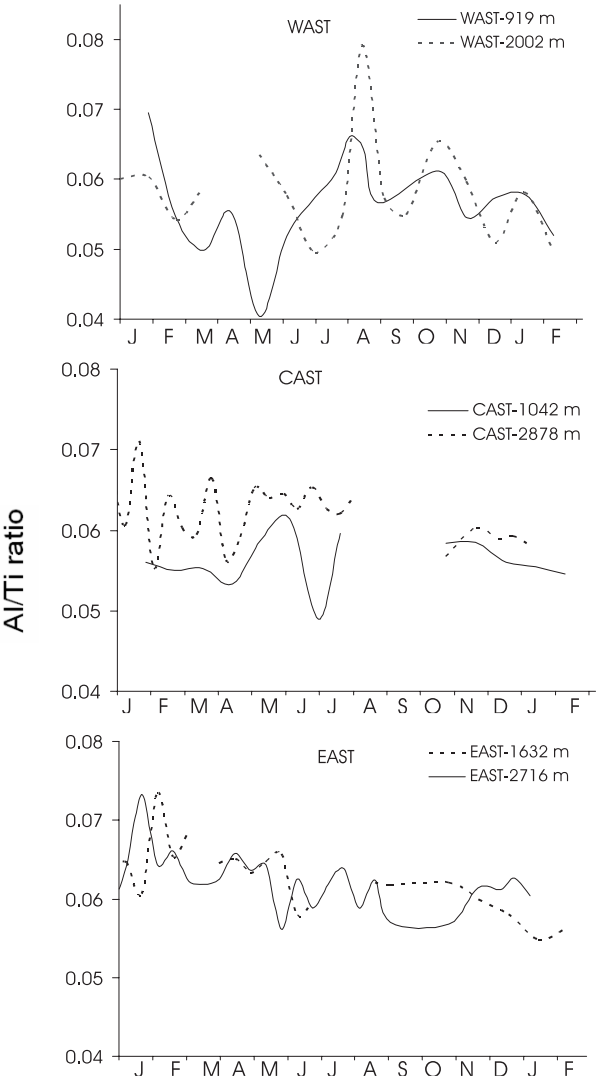

Figure 5. Seasonal variation of Ti/Al ratio in the settling particle collected from western (WAST), central (CAST) and eastern (EAST) Arabian Sea.

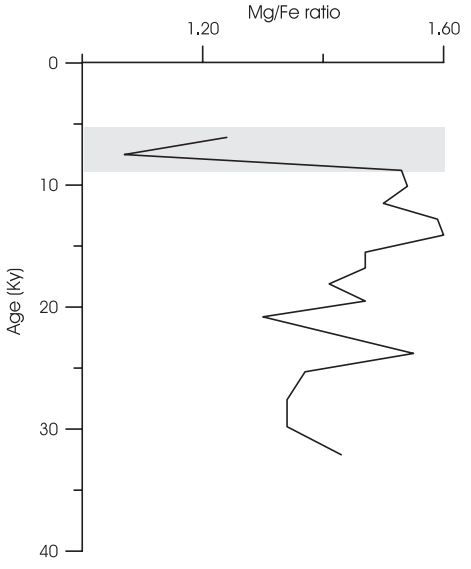

Figure 6. Variation of Mg/Fe ratio during the last 35 Ky in the ODP sediment core (722B) collected from the Owen ridge, which is located close to the WAST site. Data from Shimmield and Mowbray (1991). The stippled area represents a drastic change in Mg/Fe ratio around 8 Ky. Average Mg/Fe ratios during the SW and NE monsoons of present day are also shown.

directly linked to the strength of the transport process (Boyle 1983; Zabel *et al* 1999). Ti/Al ratios in the settling particle in the western Arabian Sea ranged from 0.04 in the intermonsoon period to ~ 0.07 in the monsoon periods (figure 5). In the central and the eastern Arabian Sea, high ratios are noticed at the end of the NE monsoon (figure 5). The peaking of Ti/Al and Mg/Fe ratios during the end of the SW monsoon indicates that the deposition of dolomite and heavy minerals containing Ti takes place during the high wind periods when the SW monsoon winds drag the westerlies from further north. Though wind speed is less during the NE monsoon, when compared to that in the SW monsoon, the wind direction is more favourable for the transportation of dolomite and heavy minerals during the former season. This is the reason for comparably higher ratios both in the SW and NE monsoon. Thus, the intensification of NE monsoon wind in the past would have caused higher deposition of dolomite and heavy minerals and thus high Mg/Fe and Ti/Al ratios. The Mg/Fe ratios in sediment cores from the western Arabian Sea should indicate intensification of the NE monsoonal winds. In order to examine this possibility Mg/Fe ratio was plotted for sediments from the ODP hole 722c located close to the WAST location (figure 6). The down-core record shows high Mg/Fe ratios around 15–25 ka B.P., i.e., the period of last glaciation (Isotope stage 2) characterized by intensification of NE monsoonal winds (Sirocko *et al* 2000). However, at ~ 8 ka B.P., Mg/Fe ratios decrease drastically, marking the lowest NE monsoonal wind velocity and intensified SW monsoon. Therefore, it is proposed that Mg/Fe and Ti/Al ratio could be a potential proxy for studying paleo-wind intensity and patterns.

Acknowledgements

I am thankful to the Director, Indian National Centre for Ocean Information Services (INCOIS) and Ministry of Ocean Development for encouragement. Dr. V Ramaswamy, NIO Goa is thanked for providing the sediment trap samples and Dr. V K Banakar, NIO Goa for ICP-AES analysis. I am grateful to Dr. V Ittekkot, University of Bremen for providing the flux data. Two anonymous reviewers are thanked for critical comments, which helped to improve the manuscript.

References

Ackerman S A and Cox S K 1989 Surface weather observations of atmospheric dust over the southwest summer monsoon region; *Meteor. Atmos. Phys.* **41** 19–34.

Al-Saayari S S and Zotl J G 1978 Quaternary period in Saudi Arabia (Wein, New York: Springer-Verlag) 334p.

Balakrishnan Nair T M, Ramaswamy V, Shankar R and Ittekkot V 1999 Seasonal and spatial variation in settling manganese fluxes in the northern Arabian Sea; *Deep-Sea Res. I* **46** 1827–1839.

Balakrishnan Nair T M, Guptha M V S, Shankar R and Ittikkot V 2005 Settling Barium fluxes in the Arabian Sea: Critical Evaluation with Export Production; *Deep-Sea Res. II* **52** 1930–1946.

Balsam W L, Otto-Bliesner B L and Deaton B B 1995 Modern and last glacial maximum eolian sedimentation pattern in the Atlantic Ocean interpreted from sediment iron oxide content; *Paleoceanography* **10** 493–507.

Boyle E A 1983 Chemical accumulation variations under the Peru Current during the past 130000 years; *J. Geophys. Res.* **88** 7667–7680.

Bruland K W, Orians K J and Cowen J P 1994 Reactive trace metals in the stratified central North Pacific; *Geochim. Cosmochim. Acta.* **58** 3171–3182.

Chester R, Berry A S and Murphy K J T 1991 The distributions of particulate atmospheric trace metals and mineral aerosols over the Indian Ocean; *Marine Chem.* **34** 261–290.

Chester R, Sharples E J and Sanders G C 1985 The concentration of particulate aluminium and clay minerals in aerosols from the northern Arabian Sea; *J. Sedim. Petrol.* **55** 37–41.

Clemens C S 1998 Dust response to seasonal atmospheric forcing: Proxy evaluation and calibration; *Paleoceanogr.* **13** 471–490.

Delany A C, Parkin D W, Griffin J J, Goldberg E D and Reimann B E F 1967 Airborne dust collected at Barbados; *Geochim. Cosmochim. Acta* **31** 885–909.

Duce R A and Tindale N W 1991 Atmospheric transport of iron and its deposition in the ocean; *Limnol. Oceanogr.* **36** 1715–1726.

Duce R A, Liss P S, Merrill J T, Atlas E L, Buat-Menard P, Hicks B B, Miller J M, Prospero J M, Arimoto R, Church T M, Ellis W, Galloway J N, Hansen L, Jickells T D, Knap A H, Rainhardt K H, Schneider B, Soudine A, Tokos J J, Tsunogai S, Wollast R and Zhou M 1991 The atmospheric input of trace species to the world ocean, *Global Biogeochem. Cycles* **5** 193–259.

Herman J R, Bartia P K, Torres O, Hsu C, Seftor C and Celarier E 1997 Global distribution of UV-absorbing aerosols from Nimbus/7 TOMS data; *J. Geophys. Res.* **102** 16,911–16,922.

Husar R B, Prospero J M and Stowe L L 1997 Characterisation of tropospheric aerosols over ocean with the NOAA advanced very high resolution radio meter optical thickness operational product; *J. Geophys. Res.* **102** 16,886–16,909.

Ittekkot V, Nair R R, Honjo S, Ramaswamy V, Bartsch M, Manganini S and Desai B N 1991 Enhanced particle fluxes in Bay of Bengal induced by injection of fresh water; *Nature* **351** 385–387.

Jickells T D, Deuser W G, Fleer A and Hemleben C 1990 Variability of some elemental fluxes in the western Tropical Atlantic Ocean; *Oceanologica Acta* **13** 291–297.

Johansen A M and Hoffmann M R 2003 Chemical characterization of ambient aerososl collected during the northeast monsoon season over the Arabian Sea: Labile-Fe (II) and other trace metals; *J. Geophys. Res.* **108** 5–10.

Khalaf F 1989 Textural characteristics and genesis of aeolian sediments in the Kuwait desert; *Sedimentology* **36** 253–271.

Konta J 1985 Mineralogy and chemical maturity of suspended matter in major river samples under the SCOPE/UNEP project; In: *Transport of carbon and minerals in major world rivers, Part 3. Mitteilungen aus dem Geologisch-Palaontologischen Institut der Universitat Hamburg* **58** 559–568.

Kumar N, Anderson R F, Mortlock R A, Froelich P N, Kubik P, Dittrich-Hannen B and Suter M 1995 Increased biological productivity and export production in the glacial Southern Ocean; *Nature* **378** 675–680.

Li F and Ramanathan V 2002 Winter to Summer monsoon variation of aerosol optical depth over the tropical Indian Ocean; *J. Geophys. Res.* **107** AAC 2-1.

Martin J H and Fitzwater S E 1988 Iron deficiency limits phytoplankton growth in the north-east subarctic Pacific; *Nature* **331** 341–343.

Mortlock R A and Froelich P N 1989 A simple method of rapid determination of biogenic opal in the pelagic marine sediments; *Deep-Sea Res.* **36** 1415–1426.

Muller G 1961 Palygorskit und sepiolith in tertiaren und quataren sedimenten von Hadramaut; *Nues Jahrbuch Mineral Abh* **97** 275–288.

Murray R W and Leinen M 1995 Scavenged excess aluminium and its relationship to bulk titanium in biogenic sediments from the central equatorial Pacific Ocean; *Geochim. Cosmochim. Acta* **60** 3869–3878.

Nair R R, Ittekkot V, Manganini S J, Ramaswamy V, Haake B, Degens E T, Desai B N and Honjo S 1989 Increased particle fluxes to the oceans related to the monsoons; *Nature* **338** 749–751.

Ramaswamy V, Nair R R, Manganini S, Haake B and Ittekkot V 1991 Lithogenic fluxes to the deep Arabian Sea measured by sediment traps; *Deep-Sea Res.* **38** 169–184.

Rixen T, Haake B, Ittekkot V, Guptha M V S, Nair R R and Schlussel P 1996 Coupling between SW monsoon-related surface and deep ocean processes as discerned from continuous particle flux measurements and correlated satellite data; *J. Geophys. Res.* **101** 28,569–28,582.

Saito C, Noriki S and Tsunogai S 1992 Particulate flux of Al, a component of land origin in the western North Pacific; *Deep-Sea Res.* **39** 1315–1327.

Schussler U, Balzer W and Deeken A 2005 Dissolved Al distribution, particulate Al fluxes and coupling to atmospheric Al and dust deposition in the Arabian Sea; *Deep-Sea Res. II* **52** 1862–1878.

Schutz L and Rahn K A 1982 Trace-element concentrations in erodible soils; *Atmos. Environ.* **16** 171–176.

Shankar R, Subbarao K V and Kolla V 1987 Geochemistry of surface sediments from the Arabian Sea; *Marine Geol.* **76** 253–279.

Shimmield G B and Mowbray S R 1991 The inorganic Geochemical record of the North West Arabian: A history of the productivity variation over the last 400 Ky from sites 722 and 724; *Proc. Ocean Drilling Program*, scientific results, pp. 409–429.

Siefert R L, Johansen A M and Hoffmann M R 1999 Chemical characterization of ambient aerosol collected during the southwest monsoon and intermonsoon seasons over the Arabian Sea: Labile Fe (II) and other trace metals; *J. Geophys Res.* **104** 3511–3526.

Sirocko F 1993 Aerosol dust in late Quaternary sediments of the Northern Indian Ocean; In: *Monsoon Biogeochemistry* (eds) Ittekkot V and Nair R R, SCOPE/UNEP International Carbon unit, University of Hamburg, pp. 185–192.

Sirocko F, Garbe-schonberg D and Devey Colin 2000 Processes controlling elemental Geochemistry of Arabian Sea sediments during the last 25,000 years; *Global and Planetary Change* **26** 217–303.

Taylor S R 1964 Abundance of chemical elements in the continental crust: A new table; *Geochim. Cosmochim. Acta* **28** 1273–1285.

Taylor S R and McLennan S M 1985 *The continental Crust: its Composition and Evolution* (Oxford: Blackwell) pp. 28.

Tindale N W and Pease P P 1999 Aerosol over the Arabian Sea: Atmospheric transport pathways and concentration of dust and sea salt; *Deep-Sea Res. II* **46** 1577–1595.

Zabel M, Bickert T, Dittert L and Haese R R 1999 Significance of the sedimentary Al:Ti ratio as an indicator for variations in the circulation patterns of the equatorial North Atlantic; *Paleoceanogr.* **14** 789–799.

Zoller W H, Gordern R A and Duce R A 1974 Atmospheric concentration and sources of trace metals at the South Pole; *Science* **183** 198–200.